MODELLING, STABILITY ANALYSIS AND DYNAMIC RESPONSE OF A MULTI-DOMAIN MECHATRONIC SYSTEM

Imran S. Sarwar, Afzaal M. Malik, Shahzad M. Sarwar
National University of Sciences and Technology, Rawalpindi, Pakistan

Corresponding Author: Imran S. Sarwar, National University of Sciences and Technology, Rawalpindi, 46000 Pakistan, College of Electrical and Mechanical Engineering, Department of Mechanical Engineering; imransarwar@ceme.edu.pk.

Abstract. This paper presents methods for the modelling and simulation of a mechatronic system such as tilt mechanism. A complete mathematical model of tilt mechanism is developed including servo actuator dynamics and presented together with dynamic simulation in this paper. The dynamic response of mechatronic system based on conventional and bond graph modelling (BGM) techniques is determined. The modelling and simulation of the mechatronic system is carried out in order to establish the strength of the BGM for the solution of coupled multi-domain mechatronic systems in a unified approach. The conventional and BGM techniques were used to obtain the state space model of the mechatronic system. The tilt mechanism design is inherently stable verified by analysis of both approaches. The motion controllers are designed and used to obtain the desired dynamic response. The performance of the tilt mechanism actuator control system is examined with numerical simulation and verified. The BGM trend matched closely with conventional model. The settling time and percentage overshoot of conventional and BGM techniques were compared that revealed the effect of distributed mass. This effect is verified by numerical simulation based on state space model and BGM technique.

1 Introduction

The paper deals with the modelling, stability analysis and motion control of a mechatronic system for positioning or aiming a camera or laser. The design of a tilt mechanism is intended to perform a tracking task. The input is described in terms of desired angular position of the camera. It is a typical case of an inverse kinematics in the sense that given a predefined object (output), the input (reference) was determined by using image processing unit (image processing software on a computing unit), we want to determine the error signal and consequently amplified error signal to the motor of the tilt mechanism.

The choice of actuator is important for the tilt mechanism. Such work [5, 9-11, 14] has presented a systematic approach to the selection of motors used in mechatronic systems. Particularly, the [5] has presented a general method for validating the size appropriateness of a selected actuating system under some predefined operating conditions based on the BGM. The [6] has discussed the actuator saturation, which is a critical limitation in choosing an actuator for a mechatronic system such as tilt mechanism. The [4] has discussed modelling and simulation of mechatronic systems and [13] has presented the model of the DC-motor using the BGM technique. The systematic way to implement the DC-motor control system is already presented in [14]. The design of pan tilt platform is already presented in [15]. The PD controller design is already presented in [3]. The pan tilt platform is a 2 degree of freedom (DOF) system that can track objects in the space and the tilt mechanism is a part of it with 1 DOF. The ability to identify and follow a moving object is important for autonomous robots used in the security applications. This can be achieved by using the pan and tilt mechanism with camera presented in [8]. The pan tilt platforms are used in many physical applications related to surveillance [3].

This paper focuses on the mechanism and actuator dynamics of the tilt mechanism. The dynamic response of pan mechanism is similar to tilt mechanism. To achieve these objectives and to verify results, two approaches are presented in this paper. First approach presented in section II of this paper is mathematical modelling of the tilt mechanism using conventional approach. The second approach using BGM of the tilt mechanism is presented in the section III. The conventional and BGM are applied to validate the response of the tilt mechanism. The gain and proportional-derivative (PD) controller were used with the models of tilt mechanism to achieve the desired response. The results are compared in section IV.

2 Conventional modelling and simulation

The dynamical model of the mechatronic system such as tilt mechanism is developed in the II (*A*). The dynamic stability analysis of the tilt mechanism is presented in the II (*B*). The dynamic response of tilt mechanism is discussed in II (C).

2.1 Modelling

The computer aided design of the tilt mechanism has been shown in figure 1 and schematic of gain compensated tilt mechanism is shown in figure 2. The tilt mechanism can rotate the device (camera) in a desired direction. To achieve the purpose, mechanism of pulleys and belt was used. The tilt mechanism is rotatable about a tilt axis supported on the pan mechanism [8, 15]. There is a pulley on the shaft of the motor as shown in figure 2. The DC motor attached with the pulley drives the mechanism. Through this mechanism of two pulleys and V-belt, the torque is transferred to the load, camera attached with pulley 2, which generates the motion. The tilt mechanism has one revolute joint with one degree of freedom.

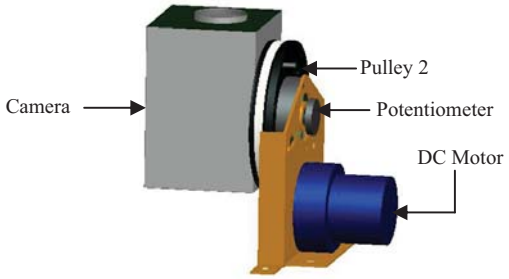

Figure 1. Tilt mechanism

The input voltage V_1, is at non-inverting end of a comparator shown in figure 2. The desired angular position (θ_i) is scaled to V_1 by using gain (K_θ). Similarly, the output is scaled to V_2 by using K_θ.

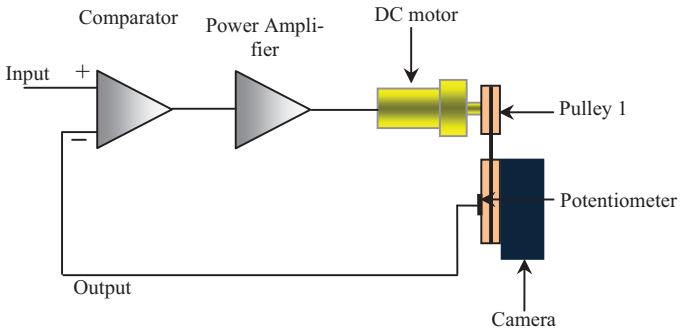

Figure 2. Schematic of gain compensated tilt mechanism

The detailed block diagram of DC motor is presented as follows

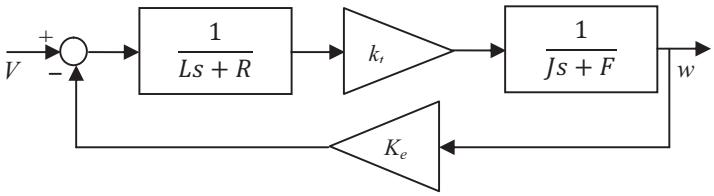

Figure 3. Block diagram of the DC motor

Thus transfer function of the DC motor is as follows

$$\frac{w}{V} = \frac{K_t}{(Ls+R)(J_a s+ f_{va})+K_t K_e} \tag{1}$$

The symbol w denotes the angular velocity of the motor shaft. The motor shaft is connected to the load through a pair of pulleys having the diameter ratio N_2 equal to n_2 / n_1, where n_1 and n_2 represents the diameters of the first and second pulley respectively. Hence the motor shaft angular velocity w and the output angular velocity of load w_o are related by

$$w_o = \frac{1}{N} w \tag{2}$$

Thus, using (1) and (2), the transfer function of the tilt mechanism is as follows.

$$\frac{w_o}{\mathrm{V}} = \frac{1}{N} \frac{\mathrm{K_t}}{(Ls+R)(J_a s + f_{va}) + \mathrm{K_t K_e}} \tag{3}$$

The tilt mechanism parameters, detail and their values are given in table I.

Parameters	Meaning	Value
K_t	Torque constant	0.0436 Nm/A
K_e	Back emf constant	0.0436 Vs
L	Armature inductance	9.35 mH
R	Armature resistance	17 Ω
J_a	Inertia of the rotor	1.6×10^{-6} kg m^2
N_1	Ratio of Gear box in front of DC-motor	6.3
N_2	Ratio between the pulleys	5.7143
f_{va}	Friction coefficient of rotor	1.4×10^{-6} Nms
J_L	Effective inertial load of pulleys and camera	0.0056 kg m^2

Table I Tilt mechanism parameters and their values

To generate power (torque × angular velocity) necessary to operate the actuator is chosen such that it follows the desired dynamics response. The block diagram of the gain compensated tilt mechanism is presented in figure 4, it is equivalent to figure 2.

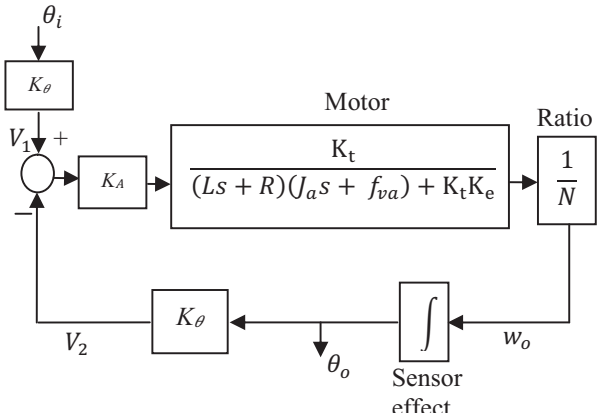

Figure 4. Block diagram of the tilt mechanism

In figure 4, the effect of the load properties does not appear in the block diagram. They are compensated in the inertia and friction of motor. The Figure 2 indicates a moment of inertias attached to the pulleys and moment of inertias for the pulleys themselves, these moments of inertia are referred to the motor shaft and incorporated in the value of J_e. Thus the equivalent inertia J_e of the tilt mechanism is equal to 9.8204×10^{-4} kg m^2. Similarly, the viscous friction associated with the output shaft could be referred to the motor and combined with f_{va}. The viscous friction f_v of the tilt mechanism is 0.00505 Nms/rad [8]. The N has a value equal to 36.0009. Now the transfer function (3) takes the form

$$\frac{w_o}{\mathrm{V}} = \frac{1}{N} \frac{\mathrm{K_t}}{(Ls+R)(J_e s + f_v) + \mathrm{K_t K_e}} \tag{4}$$

Thus, the dynamic model of tilt mechanism that follows from (4), takes the following form

$$LJ_e \ddot{w}_o(t) + (RJ_e + Lf_v)\dot{w}_o(t) + (\mathrm{R}f_v + \mathrm{K_t K_e}) w_o(t) = \frac{K_t}{N} V(t)$$

By choosing angular velocity $w_o(\mathrm{t})$ and angular acceleration $\dot{w}_o(t)$ of the load as our state variables, the 2nd-order differential equation can be expressed in state space form by introducing the state variables: $x_1 = w_o, x_2 = \dot{w}_o$ with the derivatives as $\dot{\mathrm{x}}_1 = \dot{\mathrm{w}}_\mathrm{o}, \dot{\mathrm{x}}_2 = \ddot{\mathrm{w}}_\mathrm{o}$. Thus the state equations of the tilt mechanism are

$$\dot{\mathrm{x}}_1 = \mathrm{x}_2 \tag{5}$$

$$\dot{\mathrm{x}}_2 = -\frac{(\mathrm{R}f_v+\mathrm{K_t K_e})}{LJ_e}\mathrm{x}_1 - \frac{(RJ_e+Lf_v)}{LJ_e}\mathrm{x}_2 + \frac{K_t}{NLJ_e}\mathrm{u} \tag{6}$$

Here $u = V$. The state space model in vector-matrix form is as follows

$$\dot{\mathrm{x}} = \begin{bmatrix} 0 & 1 \\ -\frac{(\mathrm{R}f_v+\mathrm{K_t K_e})}{LJ_e} & -\frac{(RJ_e+Lf_v)}{LJ_e} \end{bmatrix}\mathrm{x} + \begin{bmatrix} 0 \\ \frac{K_t}{NLJ_e} \end{bmatrix}\mathrm{u}$$
$$\mathrm{y} = [1 \quad 0]\mathrm{x}$$

Here

$$\mathrm{x} = \begin{bmatrix} x_1 \\ x_2 \end{bmatrix}, \dot{\mathrm{x}} = \begin{bmatrix} \dot{x}_1 \\ \dot{x}_2 \end{bmatrix}, \mathrm{u} = \theta_\mathrm{i}, \mathrm{A} = \begin{bmatrix} 0 & 1 \\ -\frac{(\mathrm{R}f_v+\mathrm{K_t K_e})}{LJ_e} & -\frac{(RJ_e+Lf_v)}{LJ_e} \end{bmatrix}, \mathrm{B} = \begin{bmatrix} 0 \\ \frac{K_t}{NLJ_e} \end{bmatrix}, \mathrm{C} = [1 \quad 0] \tag{7}$$

The state space model of the tilt mechanism is described by (7) and it will be compared with state space model obtained from the bond graph model of the tilt mechanism in section III.

2.2 Stability analysis

The equilibrium point of (7) is located at the (0,0) [8]. The behaviour of the tilt mechanism at equilibrium points is analyzed, to obtain the response of tilt mechanism near the equilibrium point. The function for the stability analysis of the tilt mechanism based on (7) is presented here

$$f(x) = \begin{bmatrix} \dot{x}_1 \\ \dot{x}_2 \end{bmatrix} = \begin{bmatrix} \mathrm{x}_2 \\ -\frac{(\mathrm{R}f_v+\mathrm{K_t K_e})}{LJ_e}\mathrm{x}_1 - \frac{(RJ_e+Lf_v)}{LJ_e}\mathrm{x}_2 \end{bmatrix}$$

The Jacobian at (0,0) of the tilt mechanism is as follows

$$\mathrm{A} = \frac{\partial \mathrm{f}}{\partial \mathrm{x}}\Big|_{(0,0)} = \begin{bmatrix} 0 & 1 \\ -\frac{(\mathrm{R}f_v + \mathrm{K_t K_e})}{LJ_e} & -\frac{(RJ_e + Lf_v)}{LJ_e} \end{bmatrix}$$

The eigenvalues are

$$\lambda^2 + \frac{(RJ_e + Lf_v)}{LJ_e}\lambda + \frac{(\mathrm{R}f_v + \mathrm{K_t K_e})}{LJ_e} = 0$$

Using the values of parameters presented in the table I, for the equilibrium points at (0,0) the eigenvalues are at -1818.0676 and -5.2566. Both the eigenvalues of A are negative near the equilibrium point; thus the phase portrait of tilt mechanism is a stable node.

2.3 Dynamic response

The transfer function (5) of the tilt mechanism, shown in figure 5, is developed in II (A) and simulated in the 20-sim to obtain the step response of the tilt mechanism.

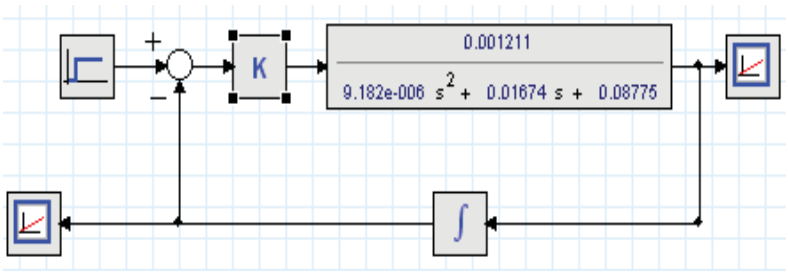

Figure 5. Gain compensated tilt mechanism

The step response of the tilt mechanism with gain compensator is shown in figure 6. Here theta_o and w_o are θ_o and w_o respectively.

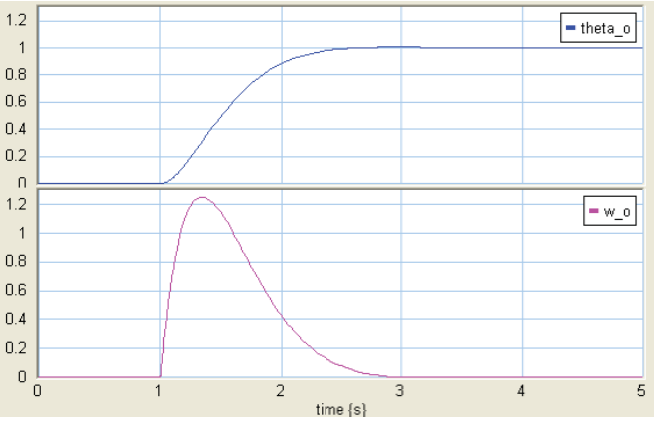

Figure 6. Step response of the tilt mechanism with gain compensator

As noticed in figure 6, we obtained the setting time, peak time and percentage overshoot equal to 1.4161 seconds (sec), 1.9802 sec and 0.5926 respectively, when the gain (K), 13.076, is selected on the intersection of the root locus and the radial line in the Matlab coding [8]. These values do not meet the desired performance values.

To compare the compensated response of conventional method with bondgraph method, we have designed the compensator for the tilt mechanism presented in figure 7. The PD controller with tilt mechanism is used to obtain desired response of tilt mechanism. In figure 7, a PD controller ($G_c(s)$) is deigned [15] according to the requirements specified [8] for the transient response and its expression is given as follows

$$G_c(s) = K(s + 12) \tag{8}$$

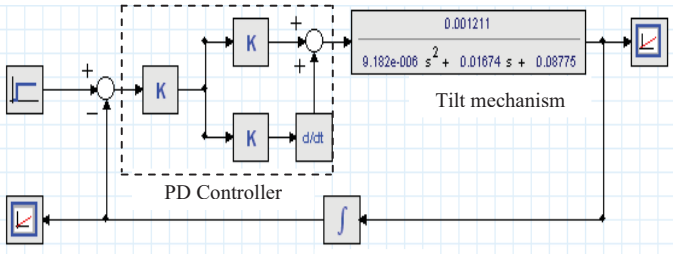

Figure 7. Tilt mechanism with PD controller

The step response of the tilt mechanism is shown in figure 7.

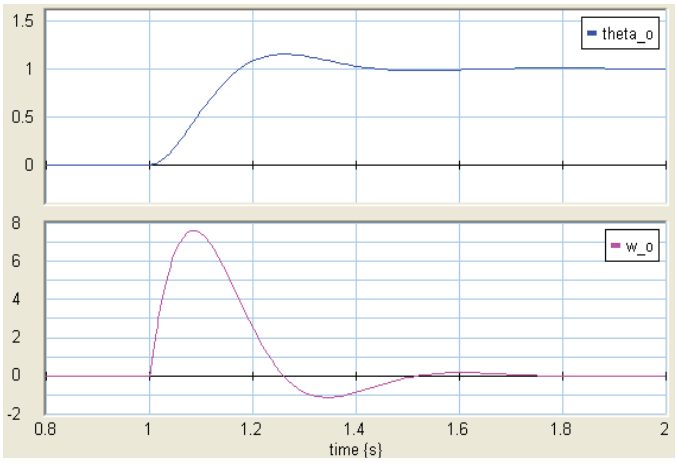

Figure 8. Step response of the tilt mechanism with PD Controller

As noticed in figure 8, the settling time, peak time and percentage overshoot equal to 0.4058 sec, 0.2614 sec and 14.8603 respectively, for the *K* equal to 13.076. These values meet the desired performance.

3 Bond graph modelling and simulation

The BGM is an emerging method for the modelling and simulation of coupled multi-domain energy systems, popularly known as mechatronic systems. The bond graph representation is a physical system based approach. This novel technique has improved modelling of mechatronic systems. The dynamic model of the tilt mechanism is developed in the III (*A*) based on BGM. The stability analysis of the tilt mechanism is presented in the III (*B*). The tilt mechanism response is discussed in III (C).

3.1 Modelling

The BGM is a precise mathematical model of the physical system in the sense that the state-space equations of the physical system can be unfolded from this BGM manually or using a simulation package, for example, 20-sim [12]. The tilt mechanism can be seen as interplay of power variables and energy variables, and thus can be used to introduce the perpetual concept of cause and effect. This research work demonstrates the methodology offered by BGM of mechatronic systems. The tilt mechanism with a feedback control system as shown in figure 9. The BGM of the tilt mechanism presented in figure 10 is obtained using a systematic construction method proposed in [1].

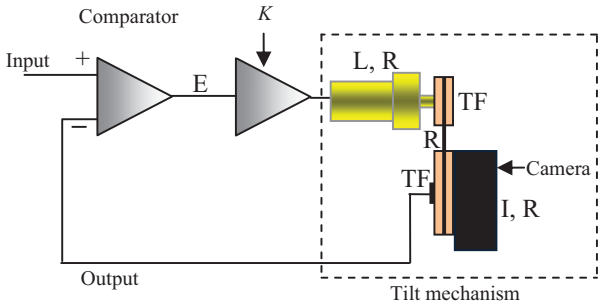

Figure 9. Gain compensated tilt mechanism with BGM elements

The pulleys ratio is used to increase the torque and decrease the speed of the motor. The BGM of the tilt mechanism is presented in the figure 10. For the mechanical rotational system such as tilt mechanism, the effort and flow are torque τ(t) and angular velocity ω(t) respectively. The following elements are used in the BGM of tilt mechanism

a. Effort source (Se),
b. Inductor and Inertia (I),
c. Resistor and viscous friction (R),
d. Transformer: pulleys ratio (TF),
e. Gyrator: motor constant (GY)
f. 0 and 1 junctions

In the linear form, the energy and co-energy variables are identified as follows.

$$f_2 = \frac{1}{I_2} p_2, f_8 = \frac{1}{I_8} p_8 \text{ and } f_{15} = \frac{1}{I_{15}} p_{15} \tag{9}$$

Here f_8 and $f_{15}$are angular velocities of the actuator and load respectively and f_2 is a current in the winding of DC motor. The p_8 and $p_{15}$are the torques of actuator and load respectively and p_2 is a voltage across the inductor. The I_8 and I_{15} are the inertias of actuator and load respectively and I_2 is a inductor in the DC motor. The state variables and input are given as follows.

$$x = \begin{bmatrix} f_2 \\ f_8 \\ f_{15} \end{bmatrix} \; and \; u = [E(t)]$$

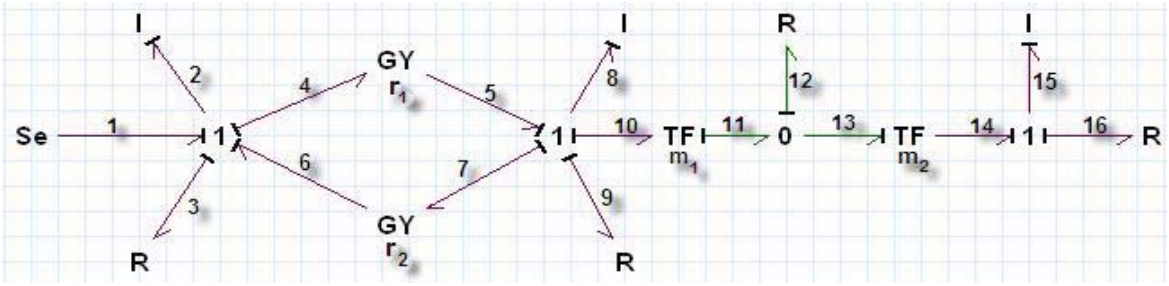

Figure 10. Bond graph model of the tilt mechanism

For p_2, p_8 and p_{15}, effort summation relation of 1-junction gives

$$\dot{p}_2 = E(t) - e_3 - e_4 + e_6 \tag{10}$$

$$\dot{p}_8 = e_5 - e_7 - e_9 - e_{10} \tag{11}$$

$$\dot{p}_{15} = e_{14} - e_{16} \tag{12}$$

The GY (r_1) and GY (r_2) have the constitutive relation

$$e_4 = r_1 f_5 \; and \; e_5 = r_1 f_4 \tag{13}$$

$$e_7 = r_2 f_6 \; and \; e_6 = r_2 f_7 \tag{14}$$

The TF (m_1) and TF (m_2) have the following relation between input and output

$$f_{10} = {f_{11}}/{m_1} \; and \; e_{11} = {e_{10}}/{m_1} \tag{15}$$

$$f_{13} = {f_{14}}/{m_2} \; and \; e_{14} = {e_{13}}/{m_2} \tag{16}$$

Using (9-16), the state equations of tilt mechanism in terms of flow variables are as follows

$$\dot{f}_2 = -\left(\frac{R_3}{I_2}\right) f_2 + \left(\frac{r_2 - r_1}{I_2}\right) f_8 + \frac{1}{I_2} E(t) \tag{17}$$

$$\dot{f}_8 = -\left(\frac{r_2 - r_1}{I_8}\right) f_2 - \left(\frac{R_9 + m_1^2 R_{12}}{I_8}\right) f_8 + \left(\frac{m_1 R_{12}}{I_8 m_2}\right) f_{15} \tag{18}$$

$$\dot{f}_{15} = \left(\frac{m_1 R_{12}}{m_2 I_{15}}\right) f_8 - \left(\frac{R_{12} + m_2^2 R_{16}}{m_2^2 I_{15}}\right) f_{15} \tag{19}$$

In the vector matrix form, these equations (17-19) can be written as

$$\dot{x} = \begin{bmatrix} -\left(\frac{R_3}{I_2}\right) & \left(\frac{r_2 - r_1}{I_2}\right) & 0 \\ -\left(\frac{r_2 - r_1}{I_8}\right) & -\left(\frac{R_9 + m_1^2 R_{12}}{I_8}\right) & \left(\frac{m_1 R_{12}}{I_8 m_2}\right) \\ 0 & \left(\frac{m_1 R_{12}}{m_2 I_{15}}\right) & -\left(\frac{R_{12} + m_2^2 R_{16}}{m_2^2 I_{15}}\right) \end{bmatrix} x + \begin{bmatrix} \frac{1}{I_2} \\ 0 \\ 0 \end{bmatrix} u \tag{20}$$

$$y = [0 \quad 0 \quad 1] x \tag{21}$$

Here

$$A = \begin{bmatrix} -\left(\frac{R_3}{I_2}\right) & \left(\frac{r_2 - r_1}{I_2}\right) & 0 \\ -\left(\frac{r_2 - r_1}{I_8}\right) & -\left(\frac{R_9 + m_1^2 R_{12}}{I_8}\right) & \left(\frac{m_1 R_{12}}{I_8 m_2}\right) \\ 0 & \left(\frac{m_1 R_{12}}{m_2 I_{15}}\right) & -\left(\frac{R_{12} + m_2^2 R_{16}}{m_2^2 I_{15}}\right) \end{bmatrix}, B = \begin{bmatrix} \frac{1}{I_2} \\ 0 \\ 0 \end{bmatrix}, C = [0 \quad 0 \quad 1], \dot{x} = \begin{bmatrix} \dot{f}_2 \\ \dot{f}_8 \\ \dot{f}_{15} \end{bmatrix}, x = \begin{bmatrix} f_2 \\ f_8 \\ f_{15} \end{bmatrix}, u = [E(t)]$$

The output y of BGM is integrated to get θ_o. The flow variables θ_o is achieved by the BGM as presented in state space model of tilt mechanism in (18-21). Thus BGM shown in figure 10 leads to state space equations; these equations have unfolded the dynamics of the tilt mechanism.

3.2 Stability analysis

The equilibrium point of (18-20) is located at $(0,0,0)$. Now we analyze the behaviour of the tilt mechanism at equilibrium point. The function for the stability analysis of the tilt mechanism based on (23) is presented here

$$f(x) = \begin{bmatrix} \dot{f}_2 \\ \dot{f}_8 \\ \dot{f}_{15} \end{bmatrix} = \begin{bmatrix} -\left(\frac{R_3}{I_2}\right) f_2 + \left(\frac{r_2 - r_1}{I_2}\right) f_8 \\ -\left(\frac{r_2 - r_1}{I_8}\right) f_2 - \left(\frac{R_9 + m_1^2 R_{12}}{I_8}\right) f_8 + \left(\frac{m_1 R_{12}}{I_8 m_2}\right) f_{15} \\ \left(\frac{m_1 R_{12}}{m_2 I_{15}}\right) f_8 - \left(\frac{R_{12} + m_2^2 R_{16}}{m_2^2 I_{15}}\right) f_{15} \end{bmatrix}$$

The Jacobian at (0,0,0) of the tilt mechanism is as follows

$$A = \frac{\partial f}{\partial x}\Big|_{(0,0,0)} = \begin{bmatrix} -\left(\frac{R_3}{I_2}\right) & \left(\frac{r_2 - r_1}{I_2}\right) & 0 \\ -\left(\frac{r_2 - r_1}{I_8}\right) & -\left(\frac{R_9 + m_1^2 R_{12}}{I_8}\right) & \left(\frac{m_1 R_{12}}{I_8 m_2}\right) \\ 0 & \left(\frac{m_1 R_{12}}{m_2 I_{15}}\right) & -\left(\frac{R_{12} + m_2^2 R_{16}}{m_2^2 I_{15}}\right) \end{bmatrix}$$

The eigenvalues of the mechatronic system are

$$\lambda^3 + \left(\frac{R_3}{I_2} + \frac{R_9 + m_1^2 R_{12}}{I_8} + \frac{R_{12} + m_2^2 R_{16}}{m_2^2 I_{15}}\right)\lambda^2 + \left(\frac{R_9 + m_1^2 R_{12}}{I_8}\frac{R_{12} + m_2^2 R_{16}}{m_2^2 I_{15}} + \frac{R_3}{I_2}\frac{R_9 + m_1^2 R_{12}}{I_8} + \frac{R_3}{I_2}\frac{R_{12} + m_2^2 R_{16}}{m_2^2 I_{15}} - \frac{m_1 R_{12}}{I_8 m_2}\frac{m_1 R_{12}}{m_2 I_{15}} + \frac{1}{I_2 I_8}(r_2 - r_1)^2\right)\lambda +$$
$$\left(\frac{R_3}{I_2}\frac{R_9 + m_1^2 R_{12}}{I_8}\frac{R_{12} + m_2^2 R_{16}}{m_2^2 I_{15}} + \frac{1}{I_2 I_8}(r_2 - r_1)^2\frac{R_{12} + m_2^2 R_{16}}{m_2^2 I_{15}} - \frac{R_3}{I_2}\frac{m_1 R_{12}}{m_2 I_{15}}\frac{m_1 R_{12}}{I_8 m_2}\right) = 0$$

The BGM of the tilt mechanism, presented in figures 10 and 11, has following parameters and their values are given in table II.

Parameters	Meaning	Value
I_2	Armature inductance of DC-motor	9.35 mH
r_1	Torque constant of DC-motor	0.0436 Nm/A
r_2	Back emf constant of DC-motor	-0.0436 Vs
R_3	Armature resistance of DC-motor	17 Ω
I_8	Rotor inertia of DC-motor	1.6×10^{-6} kg m^2
R_9	Viscous friction of DC-motor	1.4×10^{-6} Nms
m_1, m_2	Ideal transformer (Gear box and pulleys ratio) 1 and 2	1, 0.02778
R_{12}	Viscous friction due to pulleys	0.00200 Nms
I_{15}	Inertial load of the pulley with camera	0.0056 Kg m^2
R_{16}	Viscous friction of the pulley with camera	0.00305 Nms

Table II Tilt mechanism parameters and their values in the BGM

Using the values of parameters mentioned in the table II, for the equilibrium points at (0,0,0) the eigenvalues are at -1731.09481 ± 621.5940*i* and -70.1949. All the eigenvalues of *A* has real part negative near the equilibrium point; thus the phase portrait of tilt mechanism is a stable focus.

3.3 Dynamic response

The figure 9 is converted into comparable schematic diagram shown in figure 11. This equivalent and helpful in building gain compensated BGM in figure 12.

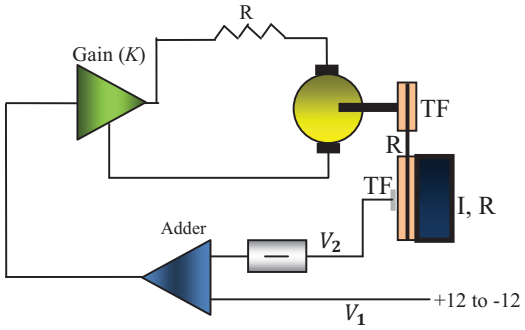

Figure 11. Schematic of gain compensated tilt mechanism with BGM elements

In figure 11 output of the comparator and amplifier is used to achieve the desired dynamic response of tilt mechanism.

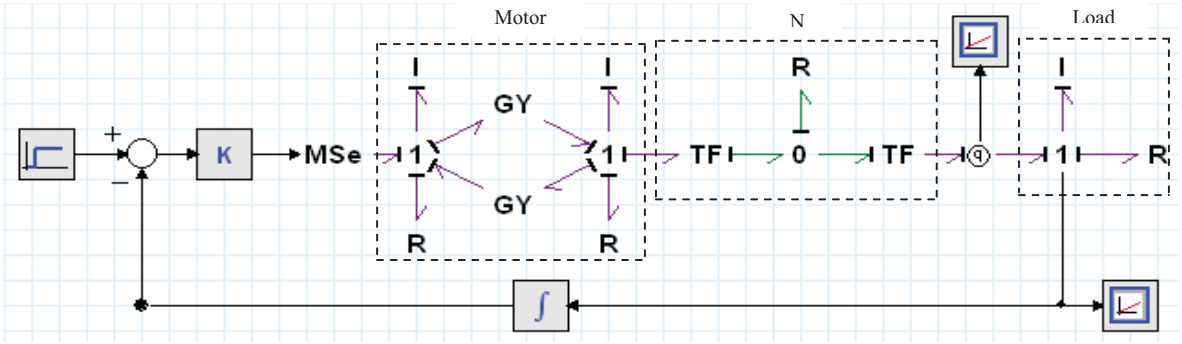

Figure 12. BGM with gain compensator

The gain compensated tilt mechanism based on BGM is presented in figs. 12. In figs. 12 and 14, MSe represents an ideal modulated effort source and flow detector q is used in the BGM to measure the angular position and angular velocity of the load. We have found linear model of the tilt mechanism using BGM in figure 10 and found its closed loop response shown in figs. 13 and 15. Similar to the section II, a BGM with gain compensation is developed and simulated using 20-sim presented in figure 12. The value of K, 13.076, was used in simulation that was obtained in section II. The step response of the tilt mechanism is shown in figure 13.

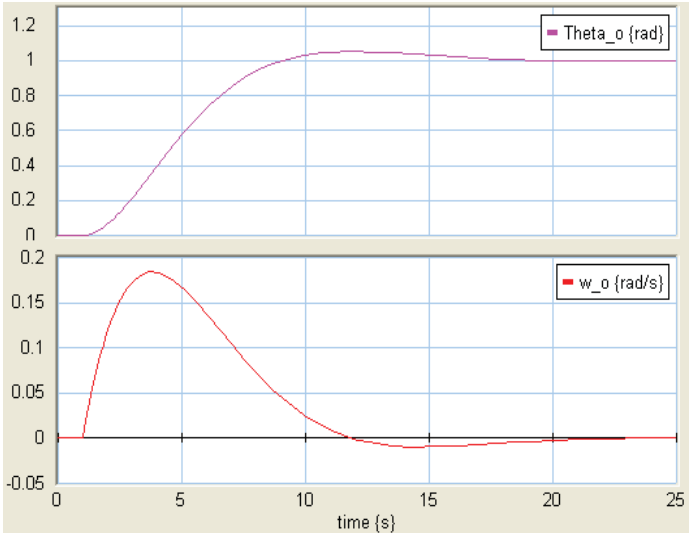

Figure 13. Step response of the tilt mechanism with *K*

As noticed in figure 13, the setting time, peak time and percentage overshoot are 15.1557 sec, 11.1019 sec and 5.1421 respectively for the gain K equals to 13.076. These values do not meet the desired performance values. Thus BGM response is about 10 times slower than the conventional model response.

This deficiency has to be compensated by designing the control system. Therefore, we have used a PD controller (8) to meet the desired performance.

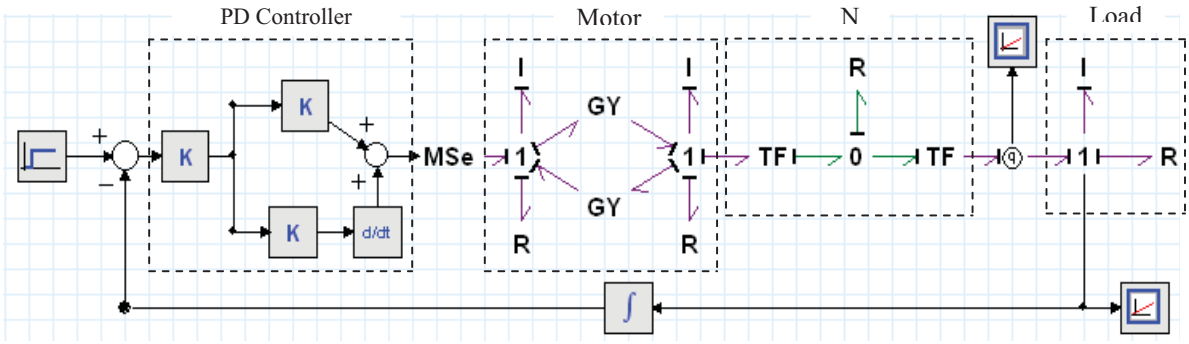

Figure 14. BGM with PD controller

The PD controller has ability to improve the transient response of the system demonstrated in section II. By using PD controller in figure 14 the transient response of BGM has improved and step response of the compensated system is shown in figure 15.

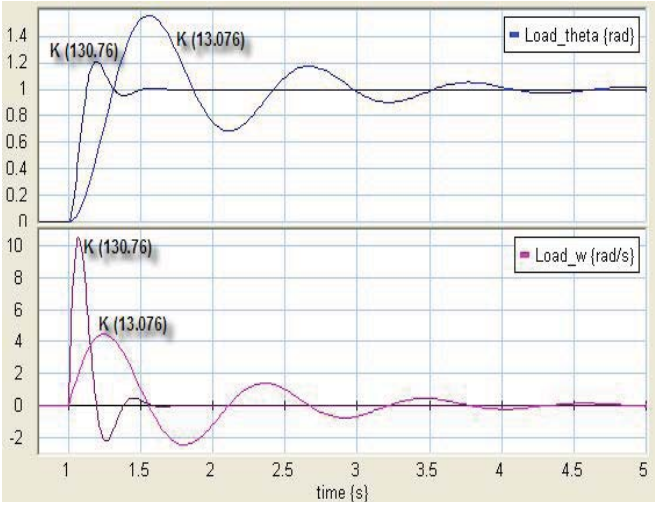

Figure 15. Step response of the PD compensated tilt mechanism

As noticed in figure 15, for the *K* equal to 13.076; the setting time, peak time and percentage overshoot are 3.5997 sec, 0.5746 sec and 55.5343 respectively. These values do not match with the values obtained in section II. As noticed in figure 15, the setting time, peak time and percentage overshoot are 0.3994 sec, 0.2393 sec and 14.2093 respectively, with *K* equal to 130.76. These values meet the desired performance value and match with the tilt mechanism with PD controller response in section II. Thus BGM response is about 10 times slower than the conventional model response.

4 Results

Both the conventional and the bondgraph methods were used for the modelling and simulation of the physical system considered. The more accurate model of the tilt mechanism was obtained using the BGM. In section III, the effect of the load parameters (inertia and friction) of the mechanism on the actuation performance was explored using the BGM. In the conventional modelling, the load characteristics (J_L, f_v) were compensated in the actuator dynamics by finding the effective load and effective friction. The state space model of the tilt mechanism was obtained using the BGM. The stability of tilt mechanism was checked the system was found stable. Thus BGM was successfully applied to the tilt mechanism and simulation of the control system was performed to achieve the desired response of the system. The values of the output θ_o of the gain compensated tilt mechanism, covered in sections II and III using con-

ventional and BGM respectively, are compared in figure 16.

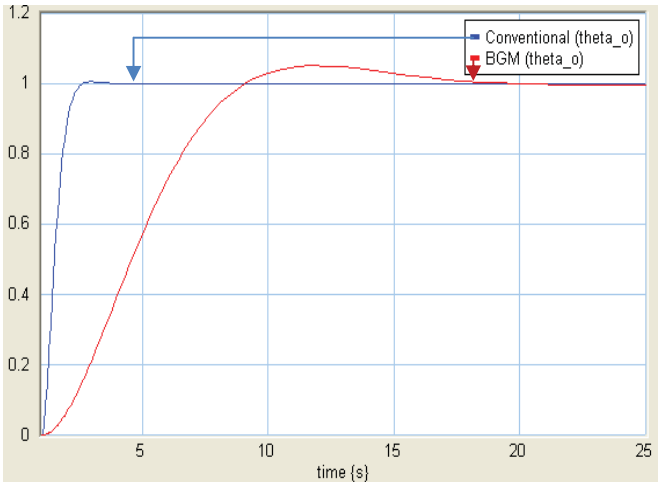

Figure 16. Comparison of the Step response of the gain compensated tilt mechanism

The comparison of the gain compensated tilt mechanism using the conventional and the BGM techniques is presented in the table III.

	Conventional modelling with *K=13.076*		**Bond graph modelling with *K=13.076***	
	***T_S* (sec)**	***%OS***	***T_S* (sec)**	***%OS***
Tilt Mechanism	1.4161	0.5926	15.1557	5.1421

Table III Comparison of Gain compensated Tilt Mechanism

The effect of load inertia and viscous friction can be explained from the results that settling time and overshoot are increased about 10 times for gain compensated BGM than gain compensated conventional model.

The comparison of the PD compensated tilt mechanism, with the conventional method and the BGM covered in sections II (C) and III (C) respectively is presented in figure 17.

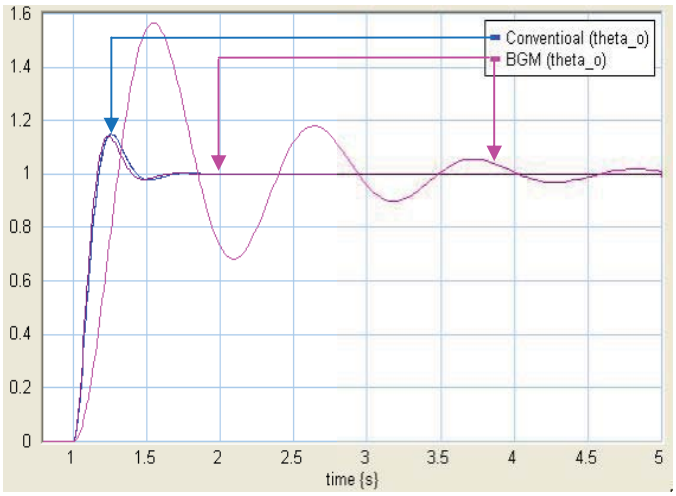

Figure 17. Comparison of the Step response of the PD compensated tilt mechanism

The comparison of the tilt mechanism with PD controller using the conventional method and the BGM is presented in the table IV.

	Conventional modelling with PD Controller		Bond graph modelling with PD Controller			
	K=13.076		*K=13.076*		*K=130.76*	
	T_S (sec)	*%OS*	T_S (sec)	*%OS*	T_S (sec)	*%OS*
Tilt Mechanism	0.405	14.86	3.599	55.53	0.399	14.20

Table IV Comparison of Tilt Mechanism with PD Controller

In the BGM the effect of inertia and friction due to pulleys and load is not combined with motor. Thus BGM is equivalent to realistic system and requires better controller to achieve the desired response. The results of compensated BGM is 10 time slower than the results of the compensated conventional model.

The efficacy of the BGM in dealing with the modelling and simulation of the mechatronic systems, that is, coupled multi-domain energy systems, has been effectively established in the application considered. This is in sharp contrast to the conventional methods which decouple the systems, or consider some average effect, thus masking the physics of the physical problem. Thus the BGM can be considered as the method of choice for the modelling and simulation of mechatronic system.

5 References

[1] Karnopp D. C., Margolis D. L., Rosenberg R. C.: *System dynamics, modeling and simulation of Mechatronic systems*, 3rd edition, John Wiley & sons, 2000, 125-250.

[2] Frederick C.: *Modeling and analysis of dynamic systems*, 2nd edition, John Wiley & sons, 1995, 529-551.

[3] Sarwar I. S., Malik A. M.: *Modeling, analysis and simulation of a Pan Tilt Platform based on linear and nonlinear systems*. In: Proc. IEEE/ASME MESA 2008, China, Oct 2008, 147-152.

[4] Malik M. A., Khurshid A.: *Bond graph modelling and simulation of mechatronic systems*. In: Proc. 7th International Multi Topic Conference, INMIC 2003, Dec 2003, 309- 314.

[5] Fotsu-Ngwompo R., Scavarda S., Thomasset D.: *Bond graph methodology for the design of an actuating system: Application to a two-link manipulator*. In: Proc. IEEE conference on computational cybernetics and simulation, vol.3, Oct 1997, 2478 – 2483.

[6] Itagaki N., Nishimura H., Takagi K.: *Two-Degree-of-Freedom Control System Design in Consideration of Actuator Saturation*. In: Proc. IEEE/ASME transactions on Mechatonics, Vol. 13 Issue: 4, Aug 2008, 470-475.

[7] Gonçalves J. B., Zampieri D. E.: *An integrated control for a biped walking robot*. In: Journal of the Brazilian Society of Mechanical Sciences and Engineering, J. Braz. Soc. Mech. Sci. & Eng. vol.28 no.4 Rio de Janeiro, Dec. 2006.

[8] Sarwar I. S., Malik A. M.: *Stability analysis and simulation of a two DOF robotic system based on linear control system*. In: Proc.15th International Conf. on Mechatronics and Machine Vision in Practice, Dec 2008.

[9] Newton G. C. Jr: *What size motor for proper operation of servomechanism?*. In: Machine Design, 1950, 125-130.

[10] Potkonjak V., Jaksic N., *Contribution to a computer-aided choice of D.C. motors for manipulation robots*, In: Robotica, Vol. 4, 1986, 37-41.

[11] Amara M., Scavarda S., Villedieu E., *Studying power transfers in the nuclear legged robot Rhesus using bond graph and scattering formalism*. In: Proc. of Int. Conf. on Bond Graph Modelling and Simulation, San Diego, California, 1993, 207-213.

[12] Controllab products B.V.: *20 Sim the power in modeling*. The Netherlands.

[13] Ferdinando. H., Warpindyasmoro. H.S.: *Developing mathematical model of DC servo motor using the bond graph*. In: 1st physics forum, Surakarta, Jul 2001.

[14] Sarwar I. S.: "*ROBOCON", Robot for the ABU Asia-Pacific robot competition, Tokyo 2002*. In: B.E. final project, Dept. Mechatronics Eng., NUST, Rawalpindi, Pakistan, 2002, 64-76, 79-86.

[15] Sarwar I. S.: *Design, modeling and control of Pan Tilt Platform for unmanned aerial vehicle*. In: M.S. thesis, Dept. Mechatronics Eng., NUST, Rawalpindi, Pakistan, 2006.